WAVE-INDUCED RESPONSE OF A 5-MODULE MOBILE OFFSHORE BASE

H.R. Riggs and R.C. Ertekin
University of Hawaii, Honolulu, HI 96822 USA

and

T.R.J. Mills
McDermott Engineering Houston, Houston, TX 77079 USA

ABSTRACT

The linear, wave-induced response of a 5-module, 1500 m long MOB is determined. Each module is a 2 pontoon, 8 column semisubmersible, and the MOB is represented by a rigid module-flexible connector model. A primary focus of the investigation is connector loads and the response mechanisms which cause them. The connector stiffness chosen for the study is considered to be realistic for a MOB. Results clearly show that the horizontal forces in the connectors are the largest, and that they are due in large measure to horizontal bending induced by oblique waves.

Key Words: Mobile Offshore Base, Connector Loads, Hydroelasticity, Fluid-structure Interaction, RMFC Model

INTRODUCTION

There has been renewed interest in floating mobile offshore bases (MOBs) for military purposes. A MOB could provide logistical support, such as the stationing of several thousand personnel and stockpiling supplies and materiel, in locales where other appropriate facilities are not available. Transport to and from the MOB would be via sea and air. Air support would require a MOB that is at least 1500 m long to accommodate large cargo airplanes.

There are several conceptual designs of a MOB. Operations in deep, unprotected waters and mobility requirements favor a multi-module design. One such design consists of conventional semisubmersible modules joined by mechanical connectors. Because semisubmersible design, analysis, and construction technologies have been well-developed and proven in the oil industry, the principle technological questions for this class of MOB relate to the connectors, including their influence on the response and the forces they must withstand.

To understand better the wave-induced behavior of multiple, connected semisubmersibles, a 5-module, 1500 m MOB has been analyzed. Each module is a two-pontoon, eight-column semisubmersible, approximately 300 m x 152 m x 72 m with an operational draft of 39 m. The modules are connected ‘serially’ with mechanical connectors near the ‘deck’ level. The primary focus of the investigation was the connector loads, and how these loads are affected by sea state and wave heading. This paper describes the analysis procedure used and presents the results of the investigation. Herein we focus on the results for one, realistic connector stiffness; a companion study focussed on the effect the connector stiffness has on the response (Riggs, et al., 1998).

A linear analysis procedure was used to determine the response. General 3-D linear hydroelasticity (Wu, 1984) admits the structurally simple rigid module-flexible connector (RMFC) model (Wang et al., 1991; Ertekin et al., 1993). In this model it is assumed that the connectors are significantly more flexible than the modules themselves, and hence all deformation occurs in the connectors. As a result, there are only 6 displacement degrees-of-freedom per module. This model is particularly useful for preliminary studies of the wave-induced motions of a multi-module MOB. Although the structural model is simplified, three-dimensional, linear potential theory can be used to include the fully coupled structure-fluid-structure interaction problem.

The connectors were modeled as linear, translational springs. The 3-D source distribution method was used to solve the coupled fluid-structure interaction problem. The frequency-dependent transfer functions for the desired response quantities were obtained in deep water for a freely floating MOB, and extreme responses for unidirectional sea-states were estimated from the transfer functions.

In the next section, the MOB design characteristics are described. Then, the analysis procedure is described, which is followed by a detailed presentation of the results.

MOB DESIGN CHARACTERISTICS

The MOB consists of 5 identical modules with a draft of 39 m. The plan dimensions of each module are 300 m x 152 m, and other principal characteristics are given in Table 1.

Table 1 Principal characteristics of a module at 39 m draft

Upper Hull	
Length	280 m
Breadth	152 m
Depth	24.6 m
Lower Hull	
Length	260 m
Breadth	38 m
Depth	16 m
Transverse Spacing	100 m
Columns	
Length	21 m
Breadth	21 m
Longitudinal Spacing	63 m
Transverse Spacing	100 m
Operational Displacement	337,000 x 10^3 kg
$\bar{I}_1$	1.0493 x 10^{12} kg-m^2
$\bar{I}_2$	2.9273 x 10^{12} kg-m^2
$\bar{I}_3$	3.1744 x 10^{12} kg-m^2
KG	26.87 m

The module properties in Table 1 are specified in a 'module' coordinate system, $\bar{x}_1 - \bar{x}_2 - \bar{x}_3$, the origin of which is located at the center of gravity (CG) of the module. Axis $\bar{x}_3$ is directed vertically up, axis $\bar{x}_1$ is directed horizontally in the longitudinal direction of the module, and axis $\bar{x}_2$ follows from the right-hand-rule. Hence, motions in the $\bar{x}_1$, $\bar{x}_2$, and $\bar{x}_3$ directions correspond to the module's surge, sway, and heave, respectively. Each module is doubly-symmetric, i.e., they are symmetric with respect to the $\bar{x}_1 - \bar{x}_3$ and the $\bar{x}_2 - \bar{x}_3$ planes.

A plan view of the MOB is shown in Fig. 1, which also defines the module numbering scheme, the global coordinate system ($x_1 - x_2 - x_3$, which corresponds to module 3's coordinate system), and the wave angle, β. Between two modules, there are two connectors, at the 'deck level.' The connectors are 'hinges,' i.e., each individual connector resists relative translational motions but not relative rotational motions. The connectors are located at $\bar{x}_2 = \pm 50$ m and $\bar{x}_3 = 33.13$ m. Longitudinally, the connectors are located 300 m on center. The connector numbering scheme is also indicated in Fig. 1, in which c_i refers to connector i.

ANALYSIS PROCEDURE

This section describes the basic theory and formulation upon which the numerical results are based. A more complete discussion of the theory can be found in Wang et al.(1991) and Ertekin et al. (1993). First, the general equations of motion for the RMFC model are discussed. Then, the hydrodynamic forces are considered, including the use of double symmetry to reduce the calculation effort. The corresponding modifications to the equations of motion are then discussed. Finally, the procedure used to estimate the extreme response in irregular seas is described.

Equations of Motion

The RMFC model has only 6 displacement degrees-of-freedom (DOFs) per rigid module. The displacements and rotations at the CG of each module are perhaps the most convenient choice for the DOFs. For the present 5-module MOB, then, the surge, sway, heave, roll, pitch, and yaw of each module compose the 30 DOFs used to represent completely the MOB motions. The displacements are ordered such that module 1's motions are displacements u_1 through u_6, module 2's motions are displacements u_7 through u_{12}, and so forth. These displacements form the 30x1 displacement vector **u**. We assume that the displacements are sufficiently small, such that linear kinematics are valid, and that the connector force-deformation relations are linear elastic. Because the linear hydrodynamic forces are most conveniently determined in the frequency domain, the equation of motion is written directly as

$$[-\omega^2 \mathbf{M}_s + i\mathbf{C}_h + (\mathbf{K}_s + \mathbf{K}_f)]\mathbf{u} = \mathbf{F}_f \tag{1}$$

and which $\mathbf{M}_s$, $\mathbf{C}_h$, $\mathbf{K}_s$, and $\mathbf{K}_f$ are the 30 x 30 structural mass, structural hysteretic damping, structural stiffness, and hydrostatic stiffness matrices, respectively, $\mathbf{F}_f$ is the 30 x 1 vector of hydrodynamic forces corresponding to each displacement DOF, and the time-harmonic dependency, $e^{i\omega t}$, has been eliminated from both sides of the equation. The structural mass and hydrostatic stiffness matrices are block diagonal matrices; the 6 x 6 submatrices are the corresponding mass and hydrostatic stiffness matrices for the corresponding rigid module. If all connectors have the same material damping ratio D, then $\mathbf{C}_h = 2D\,\mathbf{K}_s$.

The structure stiffness for the RMFC model is readily formed by assembling the stiffness for each connector. The connectors were modeled herein as discrete, 'zero-length' springs. The 'zero-length' assumption is acceptable as long as the connector dimensions are small compared to the module dimensions. The connector stiffness formulation is developed as follows. The force-deformation relationship for the springs can be written as:

$$\bar{\mathbf{F}} = \bar{\mathbf{k}}_c \bar{\mathbf{u}} \tag{2}$$

in which $\bar{\mathbf{F}} = \left[\bar{F}_{s1}\ \bar{F}_{s2}\ \bar{F}_{s3}\ \bar{M}_{s1}\ \bar{M}_{s2}\ \bar{M}_{s3}\right]$ is the vector of connector forces and moments; $\bar{\mathbf{u}}$ is the vector of corresponding deformations; and $\bar{\mathbf{k}}_c$ is a diagonal matrix with diagonals k_1 through k_6. The first 3 are translational stiffnesses, and the latter 3 are rotational stiffnesses. These relations for each connector can be transformed to the displacements of the CG of the two connected modules via a simple kinematic transformation matrix, following standard structural analysis principles.

Solution of the equation of motion, Eq. (1), requires specification of the hydrodynamic forces $\mathbf{F}_f$.

Hydrodynamic Forces

We assume the MOB is freely floating in deep water with zero forward speed. The hydrodynamic forces result from the structural motion and from a train of regular long-crested waves with frequency ω, a crest at $x_1 = 0$ (at time $t = 0$), and an incidence angle of β (see Fig. 1). The modules are partially submerged in an incompressible and inviscid fluid undergoing irrotational flow in deep water. The fluid motion is assumed small, and hence the total velocity potential, Φ, which is now a function of the spatial coordinates, can be written as

$$\Phi = \phi_I + \phi_D + \mathbf{\Phi}_R^T \mathbf{u} \tag{3}$$

ϕ_I and ϕ_D are the spatial parts of the incident and diffraction potentials, respectively. The 30x1 'vector' of radiation potentials, $\mathbf{\Phi}_R$, which represents the fluid flow caused by structural motion in an otherwise calm fluid, is

$$\mathbf{\Phi}_R = \left[\phi_1 \ \phi_2 \ \phi_3 \ \ldots \ \phi_{30}\right]^T \tag{4}$$

in which ϕ_j is the radiation potential for the jth displacement with all other displacements fixed.

The diffraction potential, ϕ_D, and the 30 radiation potentials, ϕ_j, each satisfy the Laplace equation in the fluid domain, the same linear boundary conditions on the free surface and seabed, and the Sommerfeld radiation condition on the still-water surface at infinitely large radial distances from the body. The equations are well-known; see Wang et al.(1991) and Ertekin et al. (1993) for a more complete formulation. The radiation potentials must also satisfy

$$\frac{\partial \phi_j}{\partial n} = n_j^* \quad \text{on } S \tag{5}$$

in which n represents the direction of the outward-directed unit normal vector to the wetted surface S, and n_j^* is the generalized normal, j =1,2,…,30. The generalized normal is the displacement normal to the wetted surface when $u_j = 1$ and $u_i = 0$, $i \neq j$.

The 3-D source distribution, or the Green function, method has been widely used to determine the linear flow-potential around structures of arbitrary shape. The method is well-known and is used routinely. We adopt it herein, and use the constant panel formulation of the method, to determine the potentials. Given the potentials, the hydrodynamic pressure on the wetted surface can be obtained from Euler's integral. The hydrodynamic fluid forces, $\mathbf{F}_f$, follow by integration of the hydrodynamic pressure around the mean wetted surface of the structure. The result can be written as

$$\mathbf{F}_f = (\omega^2 \mathbf{M}_f - i\omega \mathbf{C}_f)\mathbf{u} + \mathbf{F}_W \tag{6}$$

in which $\mathbf{M}_f$ and $\mathbf{C}_f$ are 30x30 fluid added mass and wave damping matrices, and $\mathbf{F}_w$ is a 30x1 vector of wave exciting forces which result from the incident and diffraction potentials. The wave exciting forces are defined by

$$F_{Wj} = i\rho\omega \int_S (\phi_I + \phi_D) n_j^* dS \tag{7}$$

in which ρ is the fluid mass density. Similarly, the terms of $\mathbf{M}_f$ and $\mathbf{C}_f$ are given respectively by

$$\mu_{ij} = \frac{\rho}{\omega} \Re \int_S \phi_i n_j^* dS \tag{8}$$

$$\lambda_{ij} = -\rho \Im \int_S \phi_i n_j^* dS \tag{9}$$

Substitution of Eq. (6) into the equations of motion, Eq. (1), results in

$$[-\omega^2(\mathbf{M}_s + \mathbf{M}_f) + i(\omega \mathbf{C}_f + \mathbf{C}_h) + (\mathbf{K}_s + \mathbf{K}_f)]\mathbf{u} = \mathbf{F}_W \tag{10}$$

Solution of Eq. (10) for a range of frequencies results in the transfer functions for the displacements. Transfer functions for the connector forces can then be determined based on these displacements.

For a MOB which is doubly-symmetric, i.e., which is structurally symmetric about the $x_1 - x_3$ and $x_2 - x_3$ planes, the double composite source distribution method (Ertekin et al., 1993; Wu et al., 1993) can be used to exploit the symmetry. The advantage to this approach, as compared to a direct application of the procedure described above, is a substantial reduction in memory requirements and computations for the hydrodynamic calculations.

Alternative-Basis Formulation

To exploit double symmetry, the displacements must be represented in doubly symmetric/antisymmetric displacement patterns, or 'modes', and then the equation of motion must be expressed in this alternative vector basis (Ertekin et al., 1993). In the previous section, surge of module 1 was represented by degree-of-freedom 1. This motion is symmetric about the plane x_1 - x_3 but it is neither symmetric nor antisymmetric about the plane x_2 - x_3. However, surge motion of module 1 can also be represented as a combination of a mode of motion involving symmetric surge of modules 1 and 5 (+surge for module 1 and –surge for module 5) and a mode involving antisymmetric surge (+surge for both modules). Modules 2, 3 and 4 have no motion in these two modes. All motions of each module can be represented similarly in terms of symmetric and antisymmetric modes. For the 5-module, 30 DOF MOB, there are 30 symmetric/antisymmetric modes, ψ_j, which contain the module displacements in mode j. The displacements $\mathbf{u}$ can be expressed as

$$\mathbf{u} = \mathbf{\Psi}\mathbf{p} \tag{11}$$

where ψ_j is column j of the transformation matrix $\mathbf{\Psi}$ and $\mathbf{p}$ is a 30x1 vector of 'generalized coordinates.'

Eq. (11), as well as the transformation for the corresponding generalized forces, $\mathbf{F}_W^*$:

$$\mathbf{F}_W^* = \mathbf{\Psi}^T \mathbf{F}_W \tag{12}$$

can be used to transform Eq. (1) to generalized coordinates:

$$[-\omega^2(\mathbf{M}_s^* + \mathbf{M}_f^*) + i(\omega \mathbf{C}_f^* + \mathbf{C}_h) + (\mathbf{K}_s^* + \mathbf{K}_f^*)]\mathbf{p} = \mathbf{F}_W^* \tag{13}$$

where

$$\mathbf{K}_s^* = \mathbf{\Psi}^T \mathbf{K}_s \mathbf{\Psi}, \quad \mathbf{M}_s^* = \mathbf{\Psi}^T \mathbf{M}_s \mathbf{\Psi}, \quad \mathbf{K}_f^* = \mathbf{\Psi}^T \mathbf{K}_f \mathbf{\Psi} \tag{14}$$

The generalized added mass and wave damping matrices are determined directly by using the generalized normal for the ψ_j modes in

Eqs. (5), (8), and (9). The generalized exciting forces are obtained by using the generalized normal for the ψ_j mode in Eq. (7).

Irregular Sea Response

The response in irregular, unidirectional seas has been determined based on the transfer functions and the Rayleigh probability distribution for the wave amplitudes. Hence, the amplitude of the short-term extreme response R_s of any quantity is given by

$$R_s = 3.72\sigma = 3.72\sqrt{m_0}, \quad m_0 = \int_0^\infty H^2(\omega) S_\eta(\omega) d\omega \tag{15}$$

in which σ is the standard deviation of the response, $H(\omega)$ is the transfer function of the amplitude-response quantity, and $S_\eta(\omega)$ is the input wave spectrum. The two-parameter Bretschneider wave spectrum has been used herein:

$$S_\eta(\omega) = \frac{1.25}{4}\frac{\omega_p^4}{\omega^5} H_s^2 e^{-1.25\left(\frac{\omega_p}{\omega}\right)^4} \tag{16}$$

where the peak wave frequency is $\omega_p = 2\pi/T_p$, and H_s is the significant wave height. Fig. 2 shows the Bretschneider spectra for the five irregular sea states that were considered for the present study (H_s = 3.25, 5.00, 7.50, 11.50, and 15.25 m and T_p = 9.7, 10.6, 12.9, 14.1 and 17.1 sec, respectively).

Panel Model

The hydrodynamic panel model of the entire wetted surface of one module at 39 m draft is shown in Fig. 3. The mesh shown involves a total of 1616 quadrilateral and triangular panels, with 80 panels on each column. However, because double symmetry was exploited, only 404 panels (and 407 nodes) were required for (one-quarter of) a single module. For one-quarter of the 5-module MOB, 2,020 panels (and 2,001 nodes) were used. This is equivalent to 8,080 panels on the entire MOB.

RESULTS

The computer program HYDRAN (OffCoast, 1998) was used to obtain the wave-induced response. The response was determined for 29 wave frequencies between 0.1 and 1.4 rad/sec. An interval of 0.05 rad/sec was used; in addition, 0.175 and 0.225 rad/sec were used in an attempt to capture possible resonance near these frequencies. Nine wave incidence angles (β = 0˚, 15˚, 30˚, 45˚, 60˚, 75˚, 80˚, 85˚, and 90˚) were considered. The near beam-sea wave angles were chosen based on previous experience with high connector loads observed in near beam seas, see Wu and Mills (1996). Results in random sea states were obtained for the 5 significant wave heights shown in Fig. 2. The results presented here focus on: 1) single module response, to compare with the MOB response; 2) fluid-structure interaction between the modules of the MOB; 3) response of a rigidly-connected MOB; and 4) response of the flexibly-connected MOB. For the latter, the connectors were modeled as translational springs, i.e., the connectors do not resist rotational deformation. The longitudinal, transverse, and vertical spring stiffnesses (k_1, k_2, and k_3) were 10^{10}, 10^{12} and 10^9 N/m, respectively. These values are considered to represent a realistic connector design. In addition, connector hysteretic damping ratios of 0, 0.5, 1, and 2% were considered. However, the response was not sensitive to the structural damping, and only undamped results will be discussed here.

Single Module

To better understand the dynamics of the 5-module MOB, it is helpful to consider the response of a single module alone (i.e., no other modules present). The RAOs (response amplitude per unit wave amplitude) are shown in Figs. 4 - 9. The resonance frequencies of the single module for heave, roll and pitch motions are estimated by using the calculated added mass and added moment of inertia for the wave frequencies. The estimated resonance frequencies are 0.193, 0.129, and 0.159 rad/sec for heave, roll, and pitch, respectively. From the RAOs, it is seen that these estimates are close, although the roll resonance is missed since we used discrete wave frequencies at 0.1 and 0.15 rad/sec. Fig. 10 shows the extreme response for the largest significant wave height considered.

Unconnected 5-Module MOB

To illustrate the degree of module-fluid-module interaction, it is convenient to compare the response of a single module with that of the MOB in which the modules are not connected. As measured by the extreme motion response in random seas, this interaction for the MOB is relatively small. It is most significant for heave and pitch in head seas. This is illustrated by comparing Figs. 10 and 11. As might be expected, in beam seas the MOB modules behave very nearly as a single module. The relatively little interaction is undoubtedly a result of the separation between adjacent module pontoons (40 m) and columns (110 m).

Rigidly Connected 5-Module MOB

From Figs. 12 and 13 it can be seen that the extreme response for a rigidly connected MOB is in general much smaller than for a single module. (As expected, near beam seas the response is very similar to the single module/unconnected MOB response.) An interesting exception is yaw at 75 degrees, for which the MOB response is larger than the single module response. The reason for this is clear if we compare the yaw RAOs for a single module and the rigid MOB (Figs. 9 and 14). Although the magnitude decreases as the wave angle increases beyond 60°, in the case of the rigid MOB the peak shifts to a higher frequency (0.35 rad/sec at 85°) at which there is significant wave energy (Fig. 2).

The second set of maximum yaw in Figs. 9 and 14, at approximately 0.7 rad/sec, are a result of the oblique wave loads on columns at opposite ends of the two pontoons. These loads depend on the oblique wave length and the distance between the opposing columns. (It is, in principle, possible to shift these maxima by changing the design in a manner similar to minimizing heave and pitch loads on a conventional semisubmersible near the peak wave frequency.) As the wave angle approaches beam seas, the maxima in yaw moments are shifted to higher frequencies. This finding is also true for the flexibly-connected MOB discussed next.

Flexibly-Connected MOB

The behavior of the MOB in yaw turns out to impact significantly the forces in the connectors. The maximum connector forces are shown in Figs. 15 – 17 for the different wave headings. It is clear the longitudinal (x_1) forces are in general substantially larger than the transverse (x_2)

and vertical (x_3) forces. We will therefore focus on these forces. As seen in Fig. 15, the connectors associated with module 3 have the highest longitudinal forces. Results for the other sea states are similar (Fig. 18). The large horizontal forces are a result almost completely of horizontal bending, i.e., relative yaw between module 3 and its adjacent modules. Consider the extreme yaw for each module (Fig. 19). Although the phase information is lacking in this figure, it indicates that module 3 yaws very little compared to the adjacent modules. This conclusion is confirmed further in Fig. 20, which shows the contribution to the horizontal force from surge, pitch, and yaw. The forces from surge and pitch almost exactly cancel each other, because they are 180° out-of-phase. This is demonstrated by the coincidence of the yaw contribution and the total RAO. Results for other wave angles (except, 0° where there is no yaw) are similar. The source of the peak in Fig. 15 at 85° can be traced to the corresponding RAOs in Fig. 21.

CONCLUSIONS

The current investigation studied the wave-induced motions and connector loads of a 5-module MOB at 39 m draft. In addition, the motions of a single module, of a 5 module rigid MOB, and 5-module unconnected MOB were also evaluated. Transfer functions and extreme responses in irregular seas were calculated. Based on the results, the following conclusions are made.

1. For a rigid MOB, the results are quite predictable. For head seas, the motions are very small. However, for beam seas the MOB behaves very much like a single module, and it loses all advantages of its size.
2. The results for an unconnected 5-module MOB reveal that the hydrodynamic interaction of the modules is small, except for heave and pitch. These motions are influenced by adjacent modules.
3. For the connector stiffness considered here, structural damping did not significantly affect the results.
4. The extreme longitudinal connector forces are significantly larger than the transverse and vertical forces for the stiffness considered here. The large forces are due almost exclusively to horizontal bending as a result of relative yaw between modules.
5. The maximum extreme connector forces occur in wave angles from 75 to almost 85 degrees. However, the assumption of long-crested random waves impinging on a 1,500 m long structure may lead to overly conservative results. There are uncertainties in assuming that the random-wave structure is spatially homogeneous over a distance of several kilometers.

ACKNOWLEDGEMENTS

The authors would like to acknowledge the support for this work by the Office of Naval Research through contract N00167-95-C-0113 to McDermott. The first and second authors also would like to acknowledge partial support by the National Science Foundation under grant BCS-9532037, and by the Office of Naval Research, MOB Program. The authors would like to thank Mr. Balakrishna Padmanabhan for his help in developing the hydrodynamic panel mesh.

REFERENCES

Ertekin, R. C., Riggs, H. R., Che, X. L. and Du, S. X., 1993, 'Efficient Methods for Hydroelastic Analysis of Very Large Floating Structures,' *Journal of Ship Research*, Vol. 37, No. 1, pp. 58-76.

OffCoast, Inc., 1998, 'HYDRAN, A Computer Program for the HYDroelastic Response ANalysis of Ocean Structures, v. 1.9.'

Riggs, H.R., Ertekin, R.C., and Mills, T.R.J., 1998, 'Impact of Connector Stiffness on the Response of a Multi-Module Mobile Offshore Base,' *Proceedings, International Offshore and Polar Engineering Conference*, Montreal, to appear.

Wang, D. Y., Riggs, H. R. and Ertekin, R. C., 1991, 'Three-Dimensional Hydroelastic Response of a Very Large Floating Structure,' *International Journal of Offshore and Polar Engineering*, Vol. 1, No. 4, pp. 307-316.

Wu, C. and Mills, T. R. J., 1996, 'Wave Induced Connector Loads and Connector Design Considerations for the Mobile Offshore Base,' *Proceedings, International Workshop on Very Large Floating Structures*, Hayama, Japan, pp. 387-392.

Wu, Y. (1984). 'Hydroelasticity of Floating Bodies,' Ph.D. dissertation, Brunel University.

Wu, Y. S., Wang, D. Y., Riggs, H. R. and Ertekin, R. C., 1993, 'Composite Singularity Distribution Method with Application to Hydroelasticity,' *Marine Structures*, Vol. 6, No. 2&3, pp. 143-163.

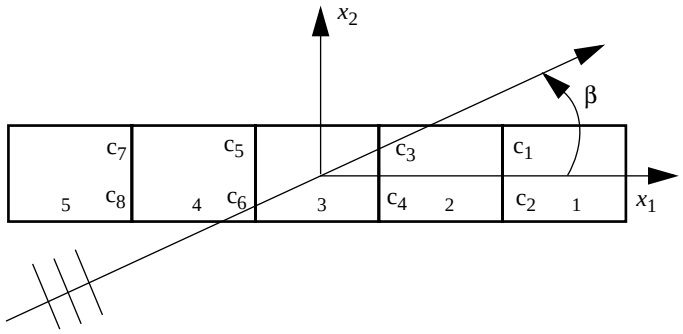

Fig. 1 Definitions of global coordinates, wave angle β, module numbers, and connector numbers

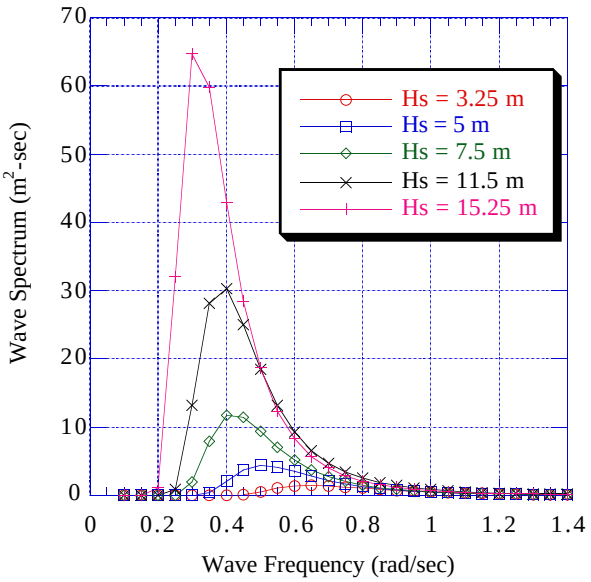

Fig. 2 Bretschneider wave spectra for five significant wave heights

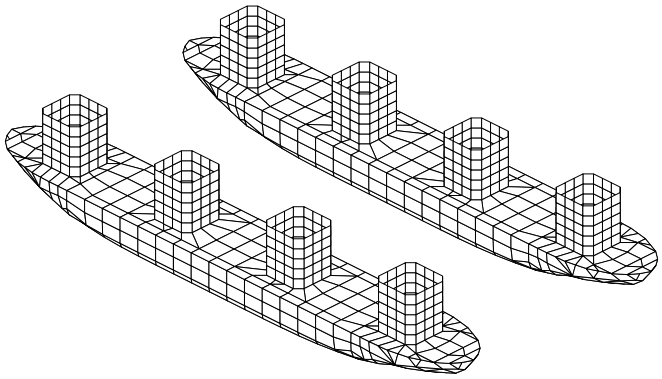

Fig. 3 A perspective view of the fluid panels for a single module

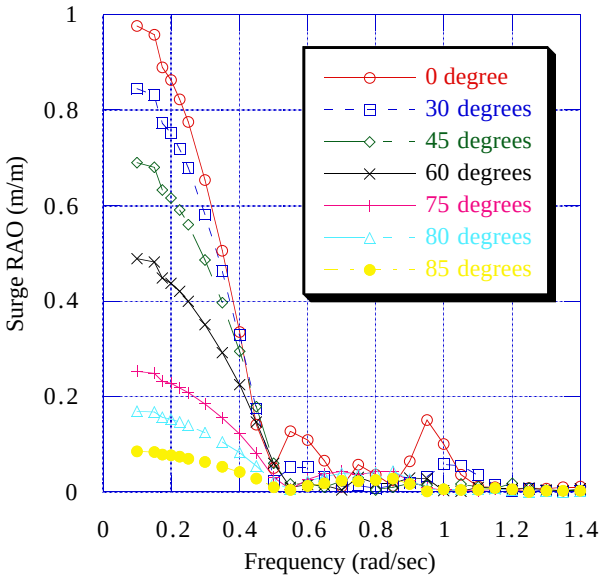

Fig. 4 Surge RAO of a single module

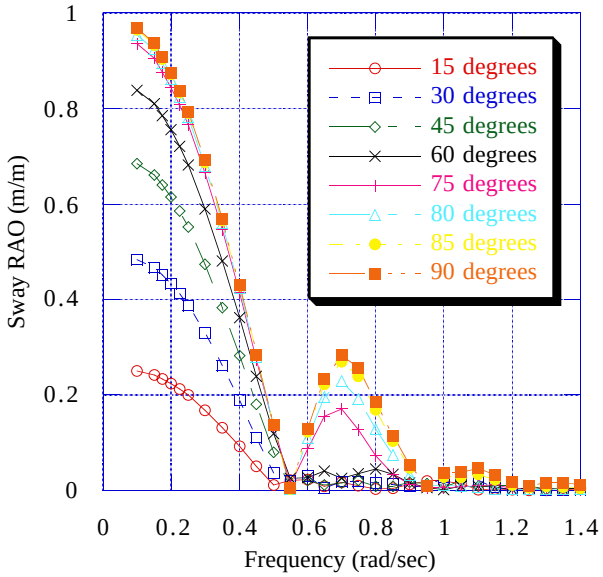

Fig. 5 Sway RAO of a single module

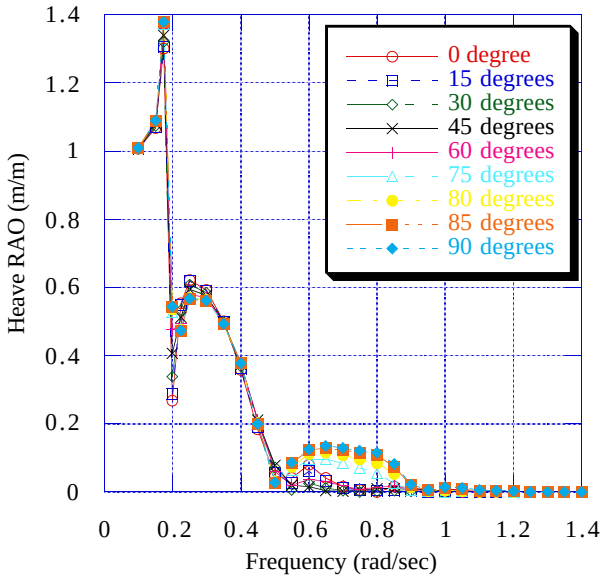

Fig. 6 Heave RAO of a single module

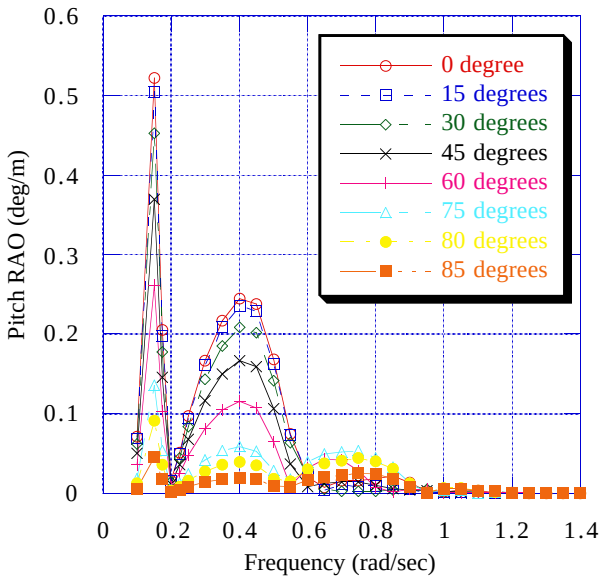

Fig. 8 Pitch RAO of a single module

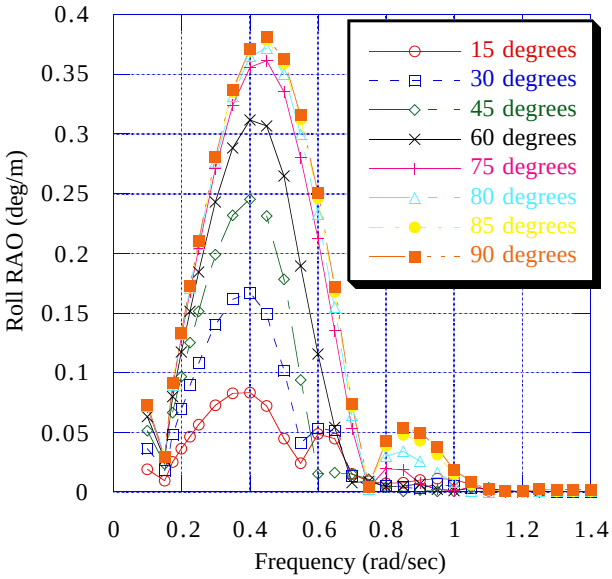

Fig. 7 Roll RAO of a single module

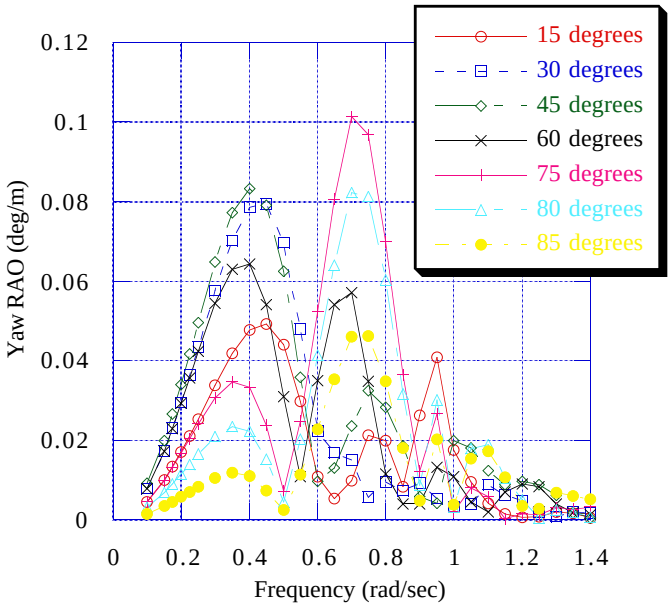

Fig. 9 Yaw RAO of a single module

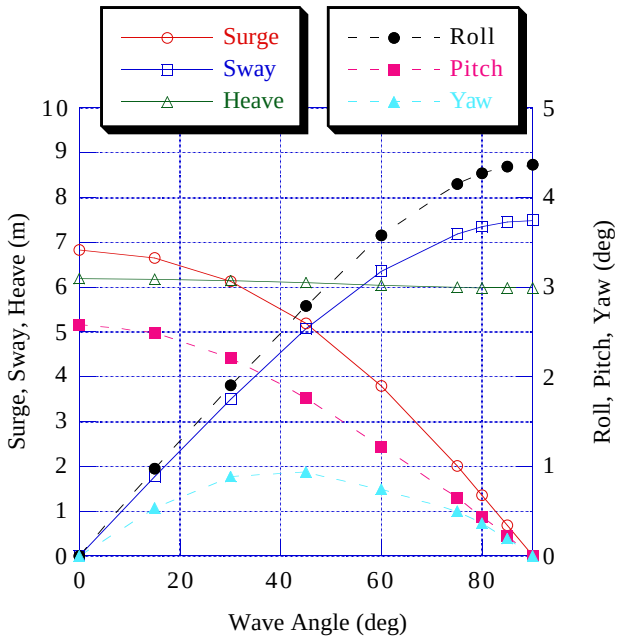

Fig. 10 Extreme response of a single module (H_S = 15.25 m)

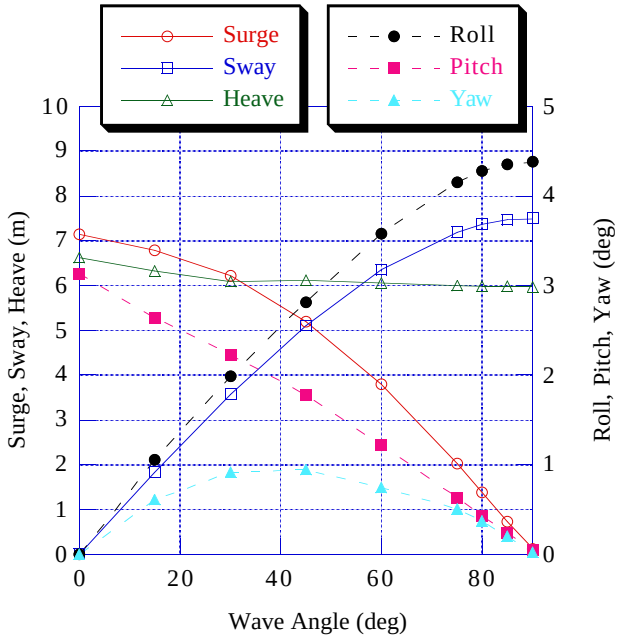

Fig. 11 Extreme module response for the unconnected MOB (H_S = 15.25 m, maximum over all modules)

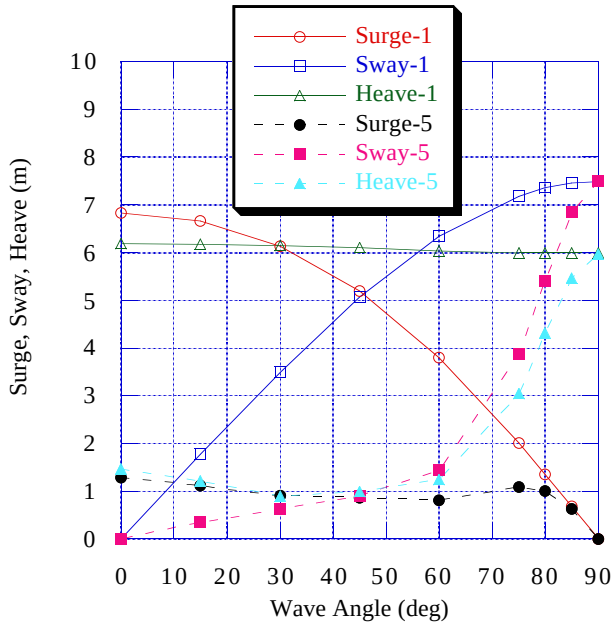

Fig. 12 Extreme surge, sway and heave for a single module and a rigid, 5-module MOB (H_S = 15.25 m)

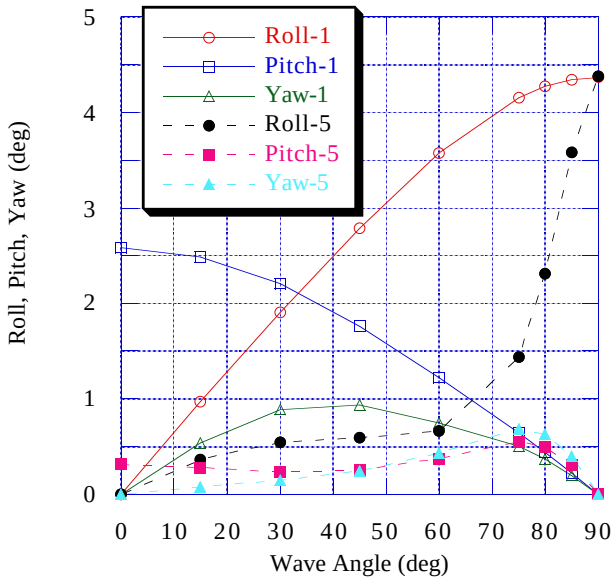

Fig. 13 Extreme roll, pitch, and yaw for a single module and a rigid, 5-module MOB (H_S = 15.25 m)

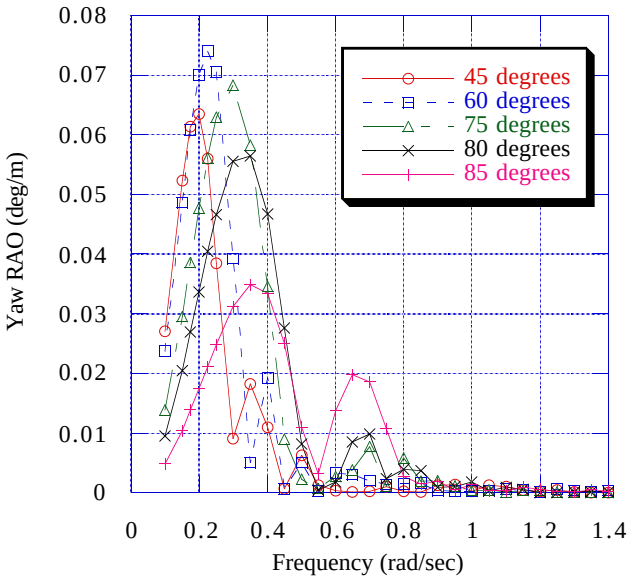

Fig. 14 Yaw RAO of the rigid MOB for 5 wave angles

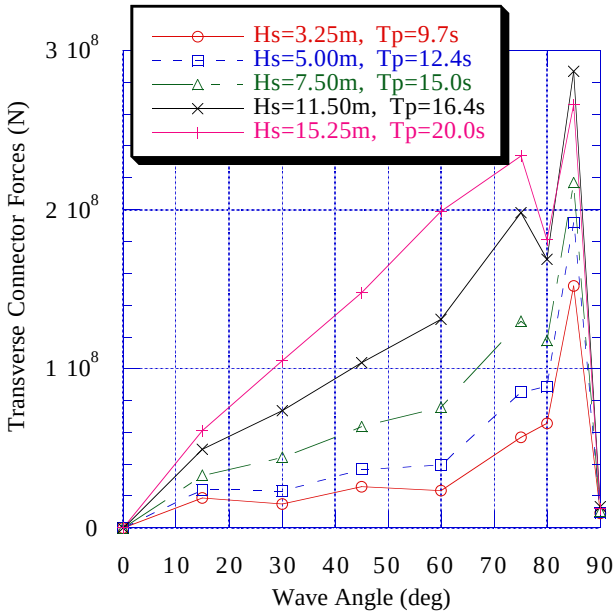

Fig. 16 Extreme transverse connector forces (H_s = 15.25 m)

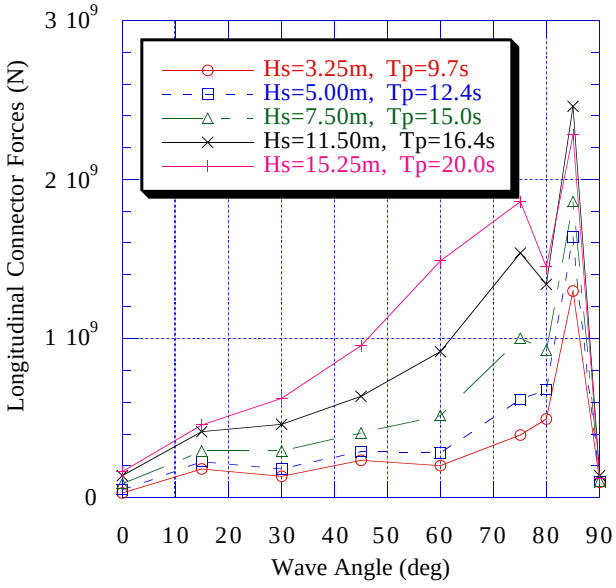

Fig. 15 Extreme longitudinal connector forces (H_s = 15.25 m)

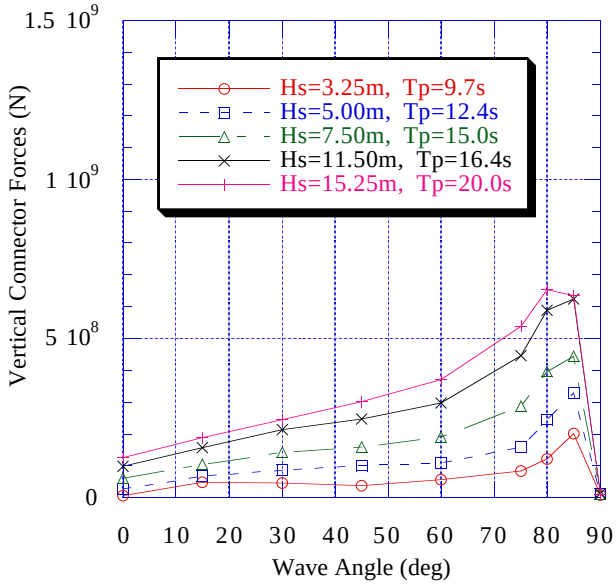

Fig. 17 Extreme vertical connector forces (H_s = 15.25 m)

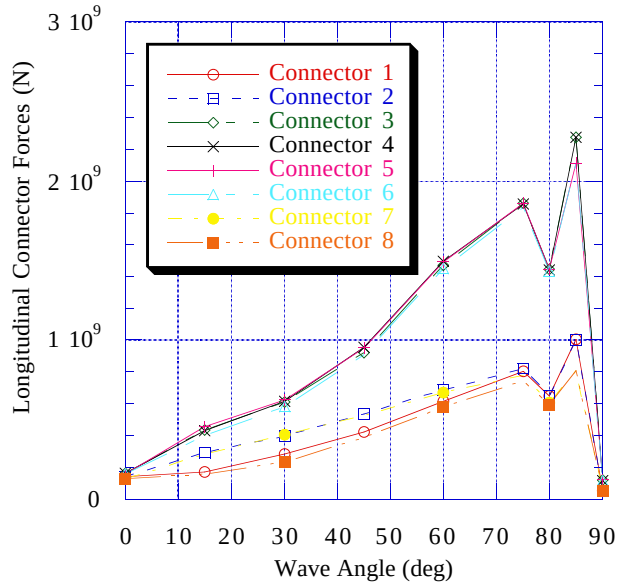

Fig. 18 Extreme longitudinal connector forces for all sea states

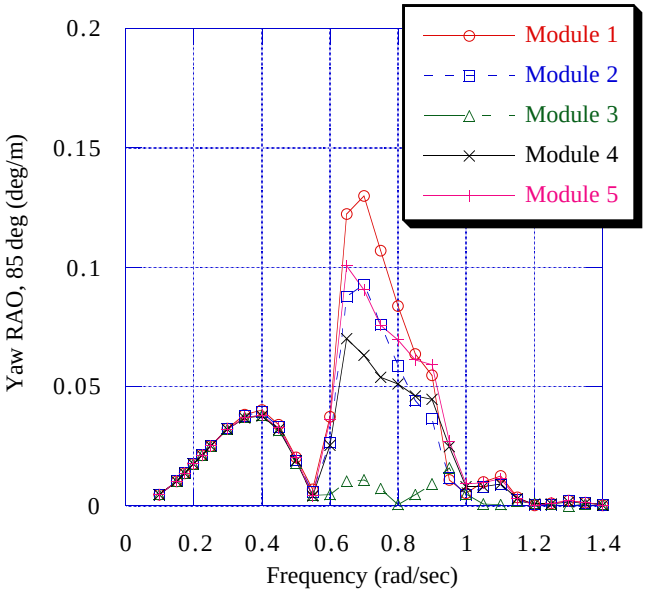

Fig. 19 Extreme yaw at 85 degree wave angle (H_s = 15.25 m)

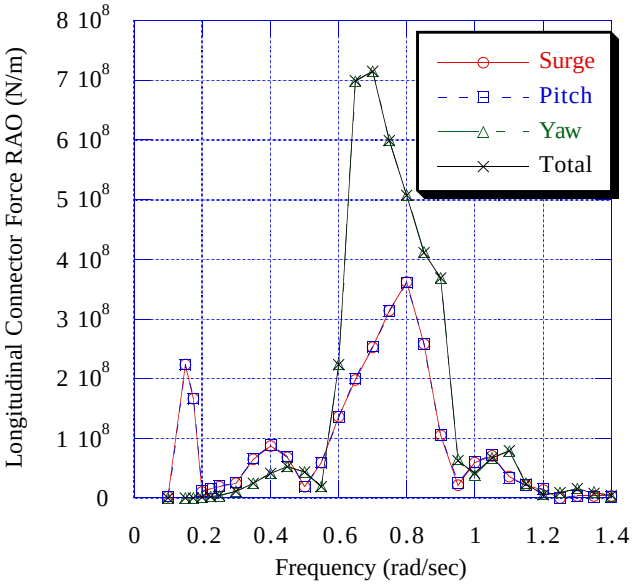

Fig. 20 RAO of longitudinal force in connector 3 at 85 degree wave angle

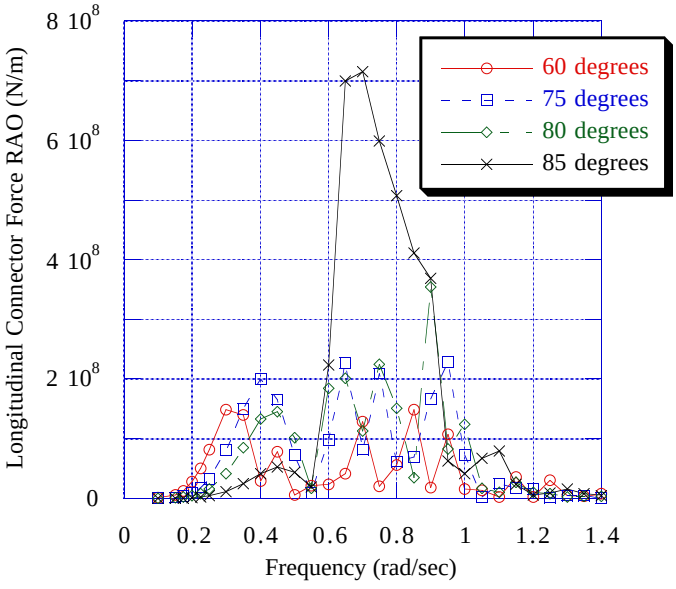

Fig. 21 RAOs of longitudinal force in connector 3